

FATIGUE EXPERIENCE FROM TESTS CARRIED OUT WITH FORGED
BEAM AND FRAME STRUCTURES IN THE DEVELOPMENT
OF THE SAAB AIRCRAFT VIGGEN

By S. E. Larsson
Saab-Scania Aktiebolag
Linköping, Sweden

2

SUMMARY

A part of the lower side of the main wing at the joint of the main spar with the fuselage frame was investigated. This wing beam area was simulated by a test specimen consisting of a spar boom of AZ 74 forging (7075 aluminum alloy modified with 0.3 percent Ag) and a portion of a honeycomb sandwich panel attached to the boom flange with steel bolts. The cross section was reduced to half scale. However, the flange thickness, the panel height, and the bolt size were full scale.

Further, left and right portions of the fuselage frame intended to carry over the bending moment of the main wing were tested. Each of these "frame halves" consisted of a forward and a rear forging (7079 aluminum alloy, overaged) connected by an outer and inner skin (Alclad 7075) creating a box beam. These test specimens were full scale and were constructed principally of ordinary aircraft components.

The test load spectrum was common to both types of specimens with regard to percentage levels. It consisted of maneuver and gust loads, touchdown loads, and loads due to ground roughness. A load history of 200 hours of flight with 15 000 load cycles was punched on a tape. The loads were randomized in groups according to the flight-by-flight principle. The highest positive load level was 90 percent of limit load and the largest negative load was -27 percent. A total of 20 load levels were used. Both types of specimens were provided with strain gages and had a nominal stress of about 300 MN/m^2 in some local areas.

As a result of the tests, steps were taken to reduce the risk of fatigue damage in aircraft. Thus stress levels were lowered, radii were increased, and demands on surface finish were sharpened.

INTRODUCTION

In designing aircraft structures against fatigue, a practice that has been used for many years at Saab can be described as follows: Reasonably low stress levels are applied and structural elements and units are carefully shaped on the basis of

load-spectrum estimates, stress analysis, fatigue testing of small specimens, and fatigue calculations. By these means costly fatigue tests on complete aircraft structures have been avoided.

After thorough consideration, this practice was also applied to the Viggen aircraft. Later, however, conditions changed: An extended service life was desired, and the static full-scale test showed a somewhat more severe stress distribution than had been predicted – in the spar boom flanges of the main wing, for example. These new conditions necessitated some sort of fatigue testing in a late development stage. In considering time, cost, the desire for easy repeatable testing, and the possibility of introducing modifications, something intermediate to conventional full-scale testing and simple (small-specimen) testing was chosen.

Before proceeding with the description of current test specimens and testing, attention should be focused on the fact that several basic fatigue studies have been done at Saab for use in the design of aircraft structures. A study of fatigue strength of aluminum lugs (ref. 1), which was presented at the 4th ICAF Symposium in Munich in 1965, can be mentioned. Block-program fatigue of riveted joints and lugs has been studied in cooperation with The Aeronautical Research Institute of Sweden (FFA). These test results, correlated with experience from the literature, have been the basis for selecting values of $\Sigma(n/N)$ for different conditions in designing. The stress engineer looks forward to data based on randomized load testing.

SYMBOLS AND UNITS

d	diameter, mm
f	life-reduction scatter factor
K_{IC}	plane-strain fracture toughness, $N/mm^{3/2}$
K_t	stress concentration factor
l	length of crack, mm
l^*	"total" length of crack (see fig. 20 for defining sketches), mm
N	number of cycles to failure at constant stress level
n	number of cycles applied at constant stress level

P	load, kN
r	notch radius, mm
T	time, h; equivalent flying time, h
T _s	service life, h
t	thickness of material, mm
v	crack propagation rate, dl^*/dT , mm/h
δ	depth of crack, mm
δ ₅	elongation, percent
ρ	root radius of milling step mark, mm
σ	normal stress, MN/m ²
σ _{max}	maximum value of stress, MN/m ²
σ _{min}	minimum value of stress, MN/m ²
σ _u	material ultimate tensile strength, MN/m ²
σ _{0.2}	0.2-percent-offset yield strength, MN/m ²

Subscripts:

y	spanwise direction
z	vertical direction

Conversion factors for the units used in this report are given in the following table:

Physical quantity	SI unit (*)	Conversion factor (**)	Customary unit
Length	meter (m)	39.4	in.
Force	newton (N)	{ 0.225	lbf
		{ 0.102	kp
Stress	MN/m ²	{ 0.145	ksi
		{ 0.102	kp/mm ²

*Prefixes to indicate multiples of units are as follows:

Prefix	Multiple
mega (M)	10 ⁶
kilo (k)	10 ³
milli (m)	10 ⁻³

**Multiply value given in SI units by conversion factor to obtain equivalent value in customary units.

AIRCRAFT PARTS AND TEST SPECIMENS

In its present design the Saab Viggen is primarily an all-weather attack aircraft. Its configuration is unconventional, with one pair of front wings and one pair of main wings.

Figure 1 shows the location of the parts that have been the object of the investigation reported: the wing beam and the fuselage frame in the main-wing region. A rear view of the wing beam and fuselage frame assembly is shown in figure 2.

A part of the lower side of the main wing at the joint of the main spar with the fuselage frame was investigated. This wing beam area, indicated in figure 2, was simulated by test specimens A₁, A₂, and A₃. Section I-I shows the aircraft design in this part, a honeycomb panel joined to the boom flange by steel bolts in two rows.

Left and right portions of the fuselage frame intended to carry over the bending moment of the main wing were also tested. These "frame halves" are denoted test specimens B₁ and B₂ in figure 2. Specimens B₃ and B₄, used in a complementary test going on when this paper was prepared, are discussed in the appendix. Section II-II in figure 2 shows the wing joint with the attachment of the two-pronged beam lugs to the forward and rear frame forging and to the intermediate part, e. The purpose of the latter component is to get some load diffusion in a compact design. Part e is not included in the test speci-

men but its attachment forces are taken into account. The upper area of the frame, made up of separate forgings, was not represented in the test.

Figure 3 shows a test specimen of type A, consisting of a spar boom of forged AZ 74 (designation according to Otto Fuchs, Metallwerke, Germany, and equal to 7075 aluminum alloy modified with 0.3 percent Ag) and a portion of a honeycomb sandwich panel attached to the boom flange with steel bolts in one row. The cross section was reduced to half scale. However, the flange thickness, the panel height, and the bolt size were full scale. The first few bolt holes in the boom flange were thought to be the most critical points, but the tests showed the flange notch to be of equal importance.

The bolted joint was provided with a sealing compound in the attachment of the panel to the boom flange. The bolts (noninterference) were treated with dry MoS₂. From the beginning the boom was anodized in a chromic acid process over its entire length, but later on, highly stressed areas were modified. They were polished and chromated (in the aircraft they are also protected by a primer). The primary boom lug for axial loading of the test specimen and the transverse lugs for stabilizing it were not representative of the aircraft structure. The limit load was 711 kN and the outer force system was nonredundant.

Geometric differences between specimens A₁, A₂, and A₃ will be referred to in the reporting of fatigue test results. The test specimen booms were taken from three separate beam forgings in almost correct positions. Their strength properties are shown in the following table (y and z denote spanwise and vertical directions, respectively):

Specimen	$(\sigma_{0.2})_y$, MN/m ²	$(\sigma_u)_y$, MN/m ²	$(\sigma_{0.2})_z$, MN/m ²	$(\sigma_u)_z$, MN/m ²
A ₁	496	551	427	491
A ₂			432	507
A ₃			427	497

The test specimens of type B are shown in figure 4. Each specimen consists of a forward and a rear forging of 7079 aluminum alloy, overaged, connected by an outer and an inner skin (Alclad 7075) creating a box beam. These test specimens were made up in full scale of essentially ordinary aircraft components.

The continuity of the outer skin is broken by a long opening in the joint area for the insert of the wing beam lugs. This is shown in section I-I and view II-II of figure 4. The inner skin has openings in the same area for the purpose of load transmission by the linkage system used in testing.

The skin was attached to the forgings mainly by countersunk aluminum screws developed for blind attachment of thick skins to extrusions and forgings. The threaded screw holes in the forgings were supposed to be critical points of the fatigue specimen. The countersunk holes in the inside Alclad sheet seemed also to be critical. Test specimens B₁ and B₂ did not include the intermediate forging (e in fig. 2). However, at the attachments a and d the test frames were clamped together with ordinary bolts and special distance elements. The frame forgings were anodized in a chromic acid process. The shear bolts in the principal lug joints (b and c) were mounted with sliced taper sleeves in bushings, which were prepared with bonded dry MoS₂.

For the right "frame half" in figure 4, forces are indicated by arrows in proper scale. The applied jack force had a limit load value of 313 kN. The force system was chosen so that joint loads correct in value and direction would be simulated at b and c, and so that the bending moment would be representative in highly stressed parts of the frame assembly.

The basic material properties of the forgings of B₁ and B₂ have not yet been determined. General material properties for 7079, overaged, can be found in the section entitled "Materials and Small-Specimen Testing."

LOAD SPECTRUM AND TEST PERFORMANCE

The load spectrum used in testing is shown in figure 5. This total spectrum, which was used for both type A and type B specimens, includes maneuver and gust loads, touch-down loads, and loads due to ground roughness. Different kinds of loads were originally presented in separate load spectra, which made up the basis for computer randomization of loads in groups according to the flight-by-flight principle. Both the severeness level of the flights and the sequence of the individual loads of the same kind were randomized.

An example of load sequences in the randomized flight-by-flight program is shown in figure 6. A load history of 200 hours of flight with 15 000 load cycles was punched on a tape for the purpose of unlimited repetitions. The highest positive load level was 90 percent of limit load and the largest negative load was -27 percent. A total of 20 load levels were used.

A diagram of the test equipment is shown in figure 7. This system was based on a modified unit for numerically controlled milling machines, a hydraulic pump with variable flow governed by the stroke, hydraulic jacks with low-friction seals of Teflon, and pressure transmitters for controlling the oil pressure in the jacks. The mean value of the frequency was 0.5 cps.

The arrangement of test specimens is shown in figure 8. The two test groups A and B were loaded by separate jacks that were only hydraulically connected. They could

work either simultaneously or separately. The somewhat odd link and lever system at the left portion of the frames in figure 8 was made up in order to get a proper redistribution of the principal outer reaction force in this part.

The test specimens were provided with strain gages for calibration and monitoring of loads. Each test started with loading to 90 percent of limit load. This load level will also be applied once during the delivery control flight of every aircraft.

Crack searches with a fluorescent penetrant (Ardrox P1) and crack-length studies were performed especially on the A specimens while loaded to 40 percent of limit load. A search for new cracks was made every 600 h. Visual observations of crack length were made more frequently but irregularly.

TEST RESULTS FROM SPECIMEN A (WING BEAM)

Table I presents a summary of test results from specimens A. The strain gages (01, 02, and 03) were applied to specimens A₁, A₂, and A₃ in the same areas. They are, however, shown only on A₂ in figure 10. From the location of the strain gages and the values in table I(a) the nominal stress at the flange notch and bolt hole 1 is estimated to have been 280 to 300 MN/m² at limit load, depending somewhat on definition.

Table I(b) shows equivalent flying hours (hours read on the punched tape) for observations of the state of cracks. Cracks 11 and 12 occurred in specimen A₁, cracks 21, 22, and 23 in A₂, and cracks 31 and 32 in A₃.

It can be seen in table I(b) that cracks appeared in specimen A₁ after only 3400 h. These cracks, no. 11, are shown in figure 9. One crack started where a radius $r = 3$ mm interacted with the principal notch radius $r = 10$ mm. Another crack started from the opposite side in a rough edge of the notch. Many very small cracks were also found in the anodized surface of the flange notch area.

The specimen in this original shape was not quite representative of the aircraft structure, and it became less representative because the specimen was modified to remove the cracked material. However, the test was continued in order to study the area with bolt holes in the boom flange – that area which originally had been thought to be the most critical. For this case the cracked material was milled off, and the shape was modified to that marked with the dashed lines. Besides cracks in areas not considered significant, no new damage was found until crack 12 appeared in bolt hole 1 at about 21 000 h. The test was finished at 24 100 equivalent flight hours without a limiting failure.

Test specimens A₂ and A₃ were like the modified form of A₁. They were polished and chromated in highly stressed boom portions.

Figure 10 shows specimen A₂ in a late stage with the cracks fully developed. Crack 21 was found after 8400 h, when it had a length of $l = 1$ mm. Its slow propagation was studied and it was under control until the test was ended as a result of bolt failure in hole 1 at 15 200 h. The crack propagation history can be followed in figure 20 (which includes sketches defining l and δ). Figure 11 shows details of the cracked specimen A₂.

Figure 12 shows fully developed cracks in specimen A₃. The nature of crack 31 was about the same as that of crack 21 in figure 10. Crack 31 was found at 7700 h, when it had a length of $l \approx 5$ mm. It propagated somewhat more rapidly than crack 21.

The most interesting crack in specimen A₃ was the crack designated 32. This crack was seen for the first time at 10 500 h (not seen at crack search 600 h earlier). When discovered it had a visible length of about 10 mm (about 12 mm was hidden under the panel). From this stage it propagated rapidly (a rate of about 0.02 mm/h) and then more slowly. The same tendency toward crack development from bolt hole 1 can be seen in figure 10. The new results, however, are the rapid propagation of crack 32 and the complicated interaction with crack 31.

Figure 13 shows the features of the locally developed fatigue fracture surfaces of the cracked area in specimen A₃. The slightly concave boom-side surface of crack 32 is thought to be the result of "Stage I" crack growth according to reference 2. The 45° direction is pronounced, and no unusual material properties or defects have been found. The surfaces were rubbed and could not give adequate information. At the stage of figure 13, crack 32 shows a tendency to change over to a 90° fatigue fracture. Figure 13 also shows that crack 32 must have been present when crack 31 passed through its area. The less interesting surfaces are not numbered.

The fatigue test of A₃ was finished at 11 700 h by a boom fracture due to fatigue cracking from the root of a transverse lug, not significant for the aircraft structure. No damage to the panel could be found in the three specimens tested.

TEST RESULTS FROM SPECIMEN B (FUSELAGE FRAME)

Table II presents a summary of test results from specimens B. Strain gages F-01 and F-02 were located on the forward frame and strain gages R-01 to R-04 were located on the rear frame. (See fig. 17 and table II(a).) Table II(a) shows frame stresses of approximately 260 to 320 MN/m² at limit load.

Table II(b) shows equivalent flying hours for occurrence of cracks and ultimate failure. The letters S, F, and R in the crack designations refer to sheet, forward forging, and rear forging, respectively. Cracks 11 to 14 occurred in specimen B₁, and cracks 21 to 23 occurred in specimen B₂.

From table II(b) it can be seen that cracks appeared at screw holes in the inner sheet of the frame assembly after 4300 equivalent flying hours. Their propagation was observed, and in some cases they were stopped by the use of a blind rivet with $d = 4.8$ mm or plug with $d = 5$ mm (sheet thickness $t = 3$ mm).

Ultimate failure of specimen B₁ occurred at 5300 h by fracture from an unexpected fatigue crack in web (1) of the rear forging, shown in figure 14. No crack search with fluorescent penetrant had been done in this area before failure. Afterward, however, four other cracks of about the same kind were indicated in three forgings of specimens B₁ and B₂. The B₂ test was also ended. An inspection made clear that the surface finish of the web areas of the milled frame forgings was worse than specified.

Figure 14 shows test specimen B₁ with fatigue cracks and the location of failure indicated. Figure 15 shows the fractured area of specimen B₁ with a sketch of the fatigue fracture surface, which represented ≈ 390 mm², or ≈ 10 percent of the whole area of the section. Figure 16 shows the surface shape of the fatigue crack that caused failure in B₁. It is representative of a number of web areas in both B₁ and B₂. The root radius ρ of the milling step marks was about 0.5 mm.

Figure 17 shows specimen B₂ with the location of cracks and strain gages indicated. Figure 18 shows the area with cracks in the inner sheet of the frame assembly. This area is not very representative of the aircraft because of the large unreinforced openings.

When the fatigue test was finished, specimen B₂ was provided with complementary strain gages for comparison with a simultaneous study of stress levels in a loaded complete fuselage. It was found that the fatigue test specimens had been loaded to stress levels about 20 percent too high in critical areas. The reasons were, in the first place, unavoidable differences between specimen and fuselage due to "skin load diffusion conditions," and in the second place, some lack of effectiveness of the frame forgings due to bad stabilization of the cross section in bending. A fourth to a half of the 20 percent difference was recovered in a modified set of specimens, B₃ and B₄, with better stabilization provided by two ordinary bulkheads, reinforcement of the inner skin, and smaller openings for the linkage system. These specimens are discussed in the appendix.

DISCUSSION

Materials and Small-Specimen Testing

A decision was made to change from the earlier standard aluminum alloy (the over-aged 7079 with Saab-Scania designation 3624-5) to AZ 74 (Saab-Scania 3633-5) as material for some primary aircraft forgings. The reason was the better resistance to stress corrosion cracking of the latter alloy. This change was made gradually, and therefore both

alloys were used in this investigation. When forgings of AZ 74 were not available for test specimens, the 7079 (overaged) was used.

The composition of the alloys and the aging conditions prescribed by Saab-Scania standard specifications are as follows:

Alloy	Zn	Mg	Cu	Ag	Aging
AZ 74	6.0	2.5	0.9	0.3	120° C for 12 to 24 h and 170° C for 4 to 7 h
7079 (overaged)	4.3	3.3	0.6		160° C for 8 h

Some material properties from Saab-Scania specifications and mean values from tests of specimens from wing beam forgings are shown in the following table (values refer to large-size forgings):

Alloy	Longitudinal direction				Transverse direction				Source of values
	$\sigma_{0.2}$, MN/m ²	σ_u , MN/m ²	δ_5 , %	K_{IC} , N/mm ^{3/2}	$\sigma_{0.2}$, MN/m ²	σ_u , MN/m ²	δ_5 , %	K_{IC} , N/mm ^{3/2}	
AZ 74	390	470	7		380	450	4		Preliminary specification
	440	510	12	1090	410	490	10	850	Test series (mean values)
7079 (overaged)	430	500	6		410	480	3		Specification, t ≤ 150 mm
	440	510	11	1010	440	500	10	780	Test series (mean values)

From the fatigue data in figure 19, which are for constant-amplitude tests, it can be seen that AZ 74 has about 10 percent higher fatigue strength than 7079 (overaged). These tests were carried out with small round specimens with diameter $d = 8.5$ mm and notch radius $r = 0.65$ mm.

Fatigue tests were also carried out with small specimens of various shapes in order to study other problems in connection with the main investigation. The aluminum blind-screw element used in specimens B (fuselage frame) was tested at constant amplitude in jointlike test pieces. Its fatigue behavior was good at stresses near limit stress but the behavior for long lives should be studied further (with regard to fretting, for example).

The "hard point effect" at bolt hole 1 in specimens A (wing beam) was simulated in a test series. A simple program of three-level tests was carried out on plain specimens "reinforced" by straps fastened to them with wing-panel attachment bolts. The intent was to find the effect of bolt fit in the boom flanges and ballizing of flange holes on the fatigue life. Ballizing was better than "easy" interference fit alone, which was better than the original small-clearance fit. However, differences were small and no change of design principle was made.

Crack Propagation and Fractures

Propagation of the cracks in the AZ 74 boom flanges of specimens A₂ and A₃ (cracks 21 and 31) is shown in figure 20. Values of l^* (total visible crack length) were plotted against the number of equivalent flying hours T . The dashed lines make up a mean curve, visually estimated. This curve indicates that crack propagation, on the average, might be slow between $T = 7000$ h and $T = 11\ 000$ h. The mean crack propagation rate is $v_1 = 0.0025$ mm/h in this time interval. (Environmental conditions, not considered in the tests, must also be accounted for when estimating the probable damage tolerance of the aircraft structure.)

The crack in specimen A₃ that caused the ultimate failure of the boom section at a nonrepresentative transverse lug had a fatigue-cracked area of ≈ 650 mm², or ≈ 25 percent of the total boom cross section. The residual strength of this section, when it failed ultimately at 83.5 percent of limit load, and that of the cracked area in specimen B₁, when it fractured at 90.1 percent of limit load, have been controlled with respect to fracture toughness behavior. Current combinations of stress levels, geometry, and K_{IC} values (from the table of material properties presented previously) could in both cases explain actual failures.

Surface Conditions and Damage

Some problems with surface roughness and anodizing as detrimental factors in fatigue of wing beam specimen A₁ were reported. Fretting was found in the boom flange of specimens A in bolt holes and on the surface that makes contact with the panel. Mainly, however, the fatigue quality of the bolt-hole area of the flange was as good as wanted. The dry film lubricant and the sealing compound have certainly been positive factors.

The main surface problem with the frame specimens B₁ and B₂ was the milling step marks shown in figure 16. In highly stressed areas, these milling marks and other surface imperfections on parts of the aircraft were eliminated by surface-improving procedures followed by adequate corrosion protection.

The test of specimen A₁ and other recent tests indicated that serious fatigue problems are sometimes associated with anodizing on aluminum parts. Thorough studies of these problems are being made.

Calculation Study

A recently developed computer method for fatigue calculations based on the linear cumulative damage theory was tested on specimens A and B and their fatigue-test results. The diagram in figure 21 shows calculated S-N curves for various K_t values based on the constant-amplitude fatigue data from figure 19, slightly reduced. The curves in figure 21 are for the specimen A material, AZ 74, the test load spectrum, and $\Sigma(n/N) = 1$. The nominal stress at limit load is plotted against calculated equivalent flying hours. The fatigue test result, $\sigma = 290 \text{ MN/m}^2$ and $T = 9000 \text{ h}$, is plotted and found to correspond to $K_t = 2.7$. (The chosen time, 9000 h, corresponds to a 5-mm fatigue crack in the flange notch, according to the mean curve in figure 20. This time, however, is also supposed to be representative for the bolt-hole cracks.)

The value $K_t = 2.7$ is larger than expected for the flange notch, but less than expected for the first and second bolt holes. This calculated result and the corresponding result for specimen B (overaged 7079 and rougher surface in the web case) are shown in the following table:

Specimen	Stress at limit load, σ , MN/m^2	T, hr	K_t	Location of crack
A	290	9000	2.7	Flange notch and bolt holes
B	280	≈5000	2.4	Web (1)
	310	>5000	<2.4	Forging inner boom

It should be noted that in the case of residual tensile stresses from heat treatment and material removal by machining, the calculation result $K_t = 2.4$ for the frame forging web will be changed. The fatigue failure corresponds to $K_t = 2.0$ if a residual tensile stress of 50 MN/mm^2 is assumed. Thus, residual tensile stresses in forgings may play a role not only in stress corrosion damage but also in fatigue life.

Stress Concentrations

Problems caused by interacting stress concentrations frequently occur in connection with forging design. Interacting notch radii in critical areas have been observed in both specimens A and B.

In order to get a better collection of data as a basis for design and for making up some estimation rules, fatigue testing has been performed and is planned to progress with specimens of various shapes. Figure 22 shows two typical configurations, representing the problem of a hole in a radius (bolt hole in a part with variable cross section) and the problem of simultaneous area variation in perpendicular planes.

Reduction Factor on Life

When testing a small number of safe-life aircraft components with proper load history, a life-reduction scatter factor of $f = 4$ is often applied to the mean test life. If specimen A, the wing-beam part of this investigation, is studied in this way, an overall service life under current test conditions can be determined. Specimen A₁, which was not representative in the flange notch area, is neglected in spite of its information about fatigue life of the bolt-hole flange area. The mean value obtained from specimens A₂ and A₃ is

$$T = \frac{1}{2}(15\ 200 + 11\ 700) = 13\ 450\ \text{h}$$

(In fact, the life of A₃ is based on a secondary-type failure.) Reduction with a factor $f = 4$ gives an overall service life of

$$T_s = \frac{1}{4}(13\ 450) = 3360\ \text{h}$$

The crack propagation rate is larger outdoors than indoors, as was observed by Schijve and De Rijk in tests on sheet specimens of 7075-T6 (ref. 3). This fact could be accounted for by using a higher reduction factor on the average time during which visible cracks exist; for example, $f = 6$ on the time after $T = 7000\ \text{h}$ (fig. 20):

$$T_s = \frac{1}{4}(7000) + \frac{1}{6}(13\ 450 - 7000)$$

$$T_s = 1750 + 1075 = 2825\ \text{h}$$

Application of test results for wing-beam specimens of type A to the real wing-beam structure of aircraft must take into consideration differences in geometry, size, and so forth. The real aircraft structure has greater three-dimensional complexity than the specimens. Therefore stress levels can differ and new points may be critical. In proper design, however, constraints reduce secondary deformations, make section areas more effective, and usually lower the stresses.

The half-scale cross section tested had full-scale flange thickness, panel height, and bolt diameter. However, the two rows of bolts actually used for panel attachment were simulated with one row only, which must be conservative according to flange bending behavior. The testing of specimens B₁ and B₂ happened to be more conservative than was originally intended (higher stresses). Consequently the fatigue life became short and further study of it by use of such things as reduction factors is without meaning.

CONCLUSIONS

The test method has turned out rather well and can be looked upon as an inexpensive and flexible alternative to conventional full-scale fatigue testing, for the purpose of structural development. However, specimens must be very carefully designed in order to represent actual load distribution on aircraft parts.

The fluorescent penetrant effectively indicated cracks at 40 percent of limit load, the inspection load used in this test.

The test results for type A (wing beam) specimens indicate an overall service life of 3360 hours if a scatter factor of 4 is applied on the mean total test life of two specimens. Many other factors, such as geometry, scale factor, and environment, could be taken into consideration.

The specimens of type B (fuselage frame) sustained a shorter total test life than the wing beam specimens. However, comparison with strain measurements on a complete fuselage showed the stress levels of the frame specimens to be too high. Further, the surface finish of the milled frame forgings happened to be worse than what is normally permitted. A new test with slightly modified specimens and load levels is going on with another two frame halves.

Attention has been focused on the problems of anodizing, surface roughness, interacting stress concentrations, and fretting.

As a result of the tests, steps were taken to reduce the risk of fatigue damage in aircraft. Thus, stress levels were lowered, radii were increased, and demands on surface finish were sharpened.

APPENDIX

WORK IN PROGRESS

A complementary fatigue test with "frame half" specimens B₃ and B₄, indicated in figure 2, is in progress as this paper is being prepared. These specimens also have forgings of 7079 (overaged). They are, relative to B₁ and B₂, constructed with better stabilization of the frame parts by two ordinary bulkheads, with reinforcement of the inner skin, and smaller openings for the linkage system. They are also polished in critical forging areas.

The test load spectrum has been slightly changed according to new conditions. Further, critical stresses are lowered 5 to 10 percent by a more favorable stress distribution in the modified specimen and 12 percent by a decrease of the jack load over the entire spectrum. Consequently, the total lowering is ≈20 percent. All these changes have been made in order to get a better load distribution with more correct stress levels for the proper simulation of aircraft structural fatigue conditions.

ACKNOWLEDGMENTS

The author is indebted to Saab-Scania Aktiebolag for permission to prepare and publish this paper. Many persons involved in the reported investigations have kindly assisted with basic data for this paper. Invaluable assistance with the preparation of the manuscript has been given by Mr. E. Persson, senior stress engineer, fatigue branch, Saab-Scania.

REFERENCES

1. Larsson, S. E.: The Development of a Calculation Method for the Fatigue Strength of Lugs and a Study of Test Results for Lugs of Aluminium. *Fatigue Design Procedures*, E. Gassner and W. Schütz, eds., Pergamon Press, Inc., c.1969, pp. 309-342.
2. Forsyth, P. J. E.: *The Physical Basis of Metal Fatigue*. Blackie & Son, Ltd. (London), 1969.
3. Schijve, J.; and De Rijk, P.: *The Crack Propagation in Two Aluminium Alloys in an Indoor and an Outdoor Environment Under Random and Programmed Load Sequences*. NLR-TR M.2156, Nat. Lucht- Ruimtevaartlab. (Amsterdam), Nov. 1965.

TABLE I.- SUMMARY OF TEST RESULTS FROM SPECIMENS A (THE WING BEAM)

(a) Strain-gage results

Stress at limit load, σ , MN/m ² , for specimen -	Strain-gage no.			Strain-gage location (shown in fig. 10)
	A1	A2	A3	
341	308	300	01	Beam at notch, 7 mm from edge, outer side
298	298	292	02	Beam at hole 1, 6 mm from step, mean value
269	286	271	03	Flange between holes 1 and 2, outer side

(b) History of cracks

Figure no.	Crack no.	Equivalent flying hours for specimen -			Comments
		A1	A2	A3	
9	11	(3400)			Geometry and surface finish not representative. Cracks occurred at flange (principal notch radius $r = 10$ mm). Cracks were removed and shape of specimen was modified.
10 and 11	21		8 400 15 200		Modified shape and polishing. Small crack found, $l \approx 1$ mm. Crack increased to $l = t = 12$ mm, $\delta = 6.0$ to 11.5 mm.
12 and 13	31			7 700 10 500 11 600	Modified shape and polishing. Small crack found, $l \approx 5$ mm. Several cracks joined in one, $l = t = 12$ mm, $\delta = 3$ to 4 mm. Crack propagated to $\approx 45^\circ$, $l = t$, $\delta = 14$ to 16 mm.
9	12	≈ 21 000			Crack in flange in edge of bolt hole 1, $\delta = 2$ mm max., fretting.
10	22		15 200		Two cracks $\pm 45^\circ$ in flange at bolt hole 1, $l \approx 2$ mm $\approx 0.5t$.
12 and 13	32			10 500 11 100	Crack out from flange at bolt hole 1, ≈ 10 mm visible. Propagated ≈ 3.5 mm, then nonpropagating.
10 and 11	23		15 200		Crack through t in flange at bolt hole 2; crack through $\approx 0.5t$ in flange at bolt hole 9.
-----	---	24 100	15 200	11 700	Testing ended. No failure or secondary-type failure.

TABLE II.- SUMMARY OF TEST RESULTS FROM SPECIMEN B (THE FUSELAGE FRAME)

(a) Strain-gage results

Stress at limit load, σ , MN/m ² , for specimen -	Strain-gage no.		Strain-gage location (shown in fig. 17)
	B ₁	B ₂	
---		*286	Sheet } Boom } Section through upper wing-joint hole of forward frame
323		299	
---		*312	Sheet } Boom } Section through upper wing-joint hole of rear frame
308		323	
---		277	Web (1) } Web (2) } Principal stress on rear side \approx 13 mm from corner with radius of 15 mm
---		255	

*Mean value over sheet thickness.

(b) History of cracks

Figure no.	Crack no.	Equivalent flying hours for specimen -		Comments
		B ₁	B ₂	
18	S-11	4300		Inner sheet of frame assembly; cracks from two screws, $l = 3$ to 5 mm visible. Cracks at three holes, $l = 4$ to 10 mm, stopped at two.
		4800		
18	S-21		4300 4800	Inner sheet of frame assembly; cracks from one screw, $l = 1$ to 3 mm visible. Cracks from three screws, $l = 2$ to 5 mm visible.
14	F-12	5300		Forward forging, web (1); corner crack from milling step mark, $l \approx 30$ mm.
17	F-22		5300	Forward forging, web (1); corner crack from milling step mark, $l \approx 15$ mm.
17	F-23		5300	Forward forging, web (2); corner crack from milling step mark, $l \approx 10$ mm.
14 to 16	R-13	5300		Rear forging, web (1); failure due to crack, $l \approx 30$ mm, in corner.
14	R-14	5300		Rear forging, web (2); corner crack from milling step mark, $l = 19$ mm.

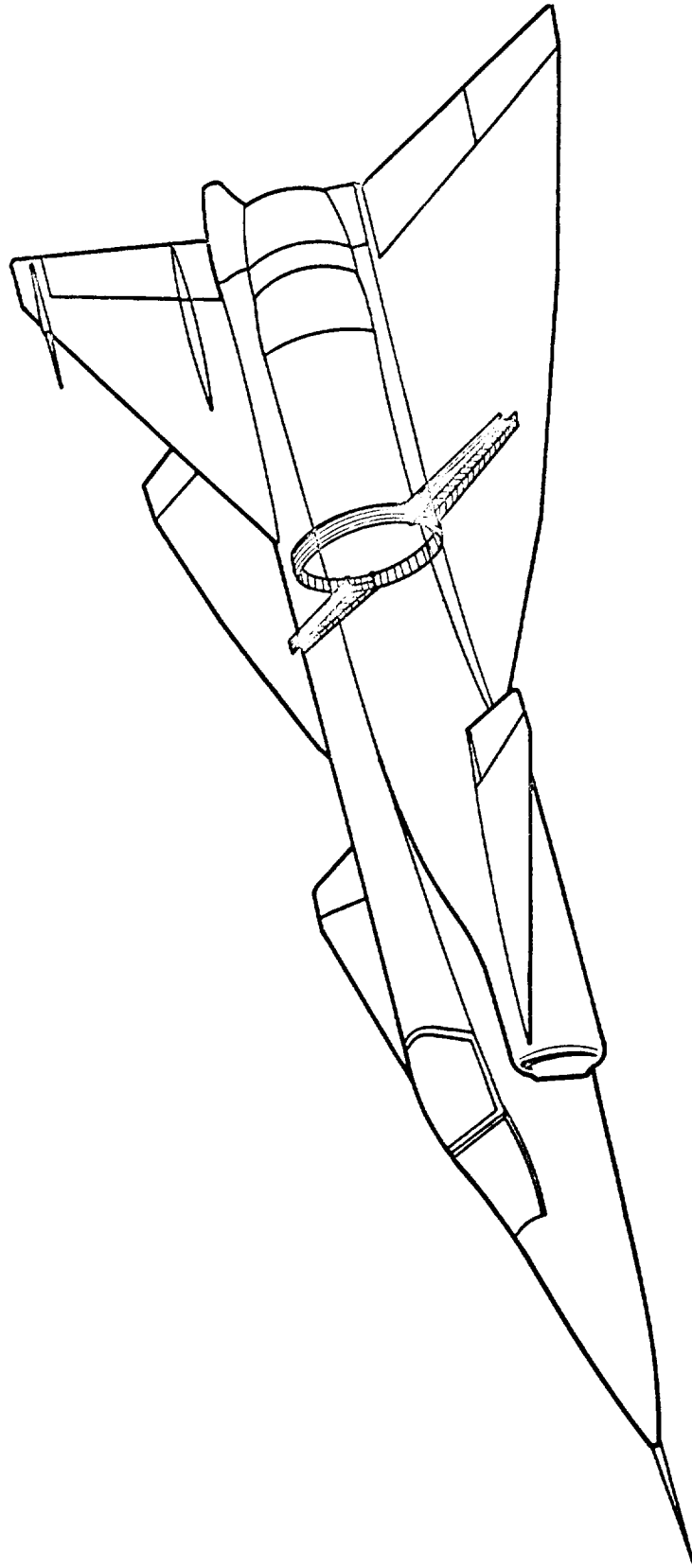


Figure 1.- Location of wing beam and fuselage frame in the Viggen aircraft.

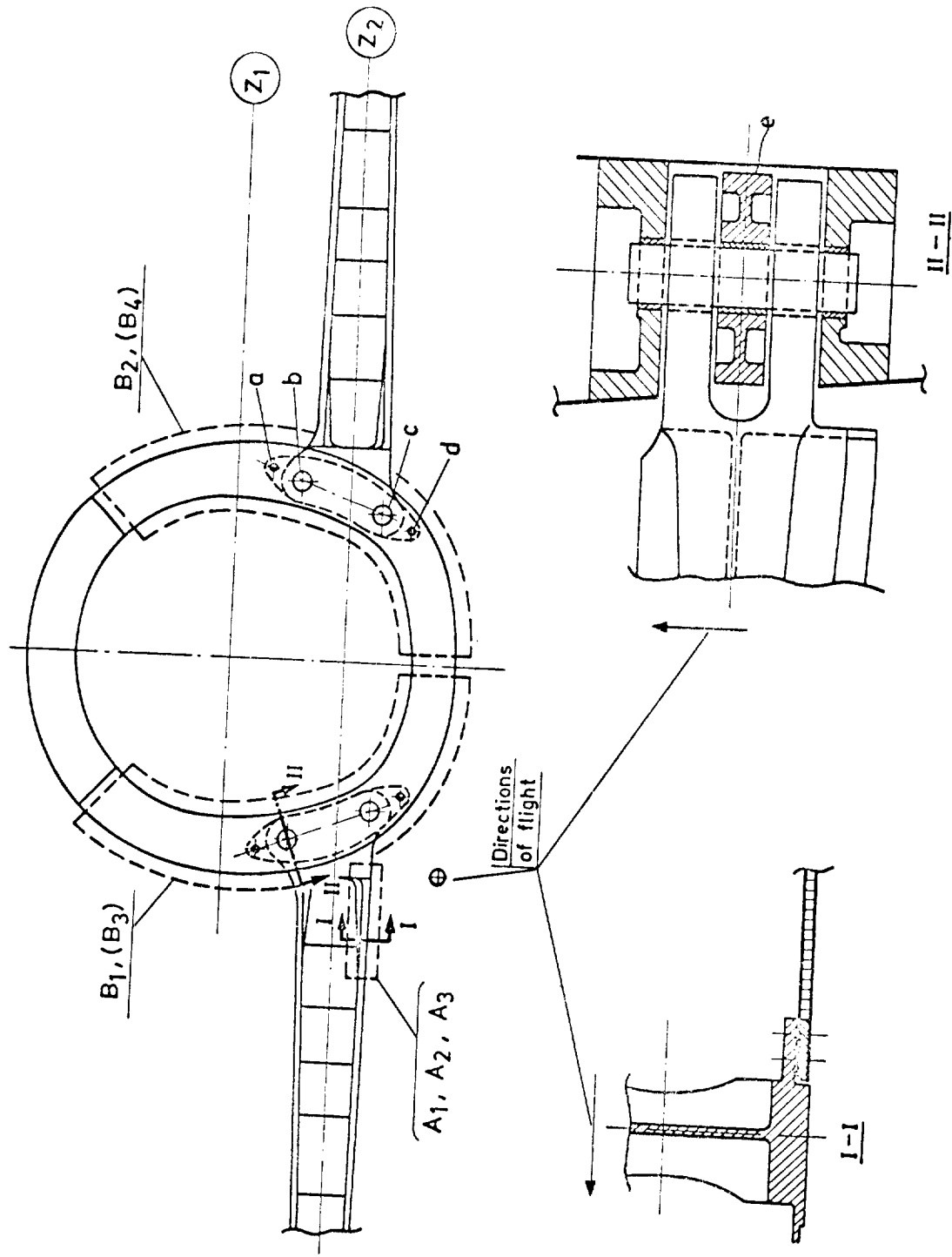


Figure 2.- Rear view of wing beam and fuselage frame assembly.

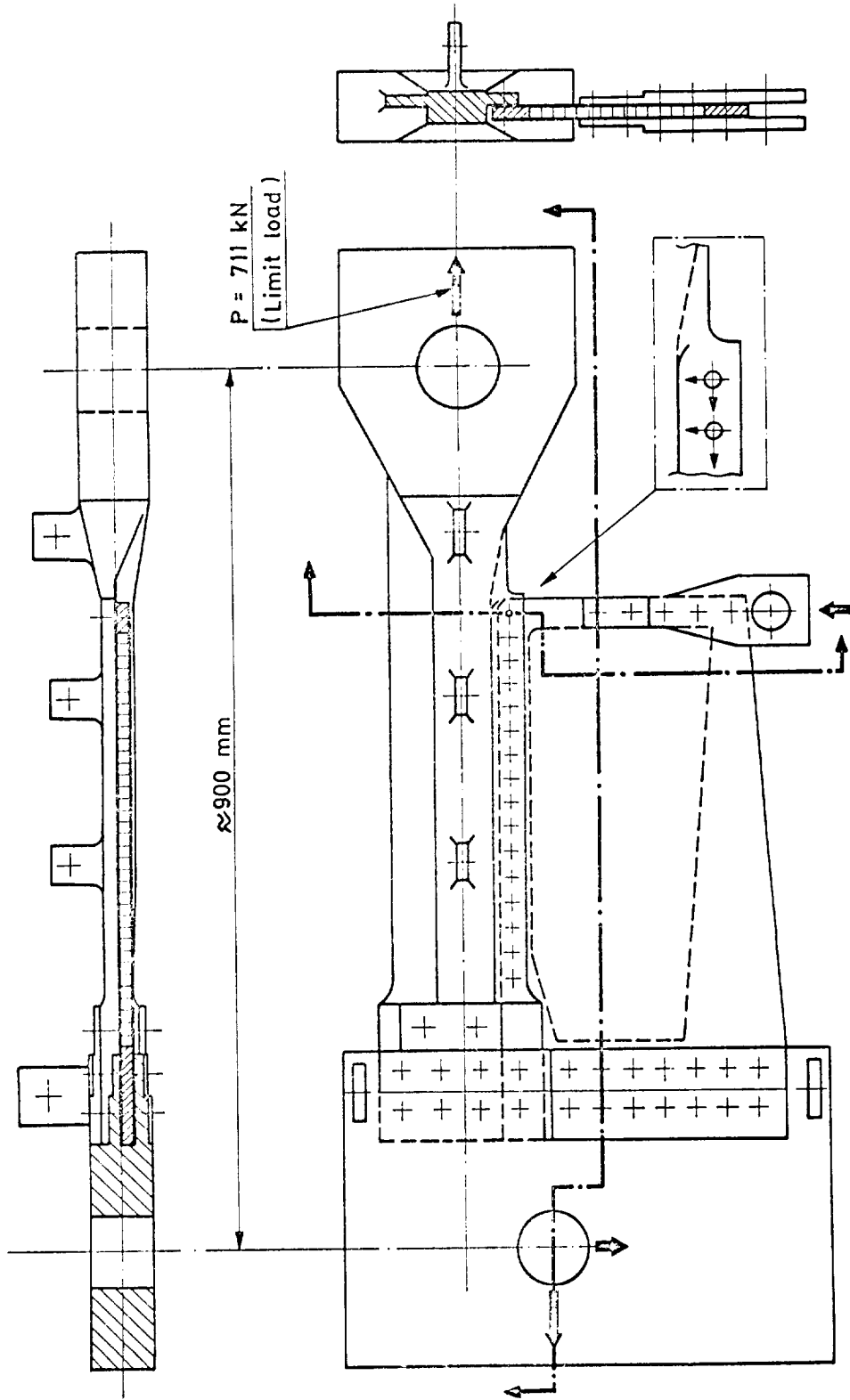


Figure 3.- Test specimen A with forces indicated by arrows.

C.3

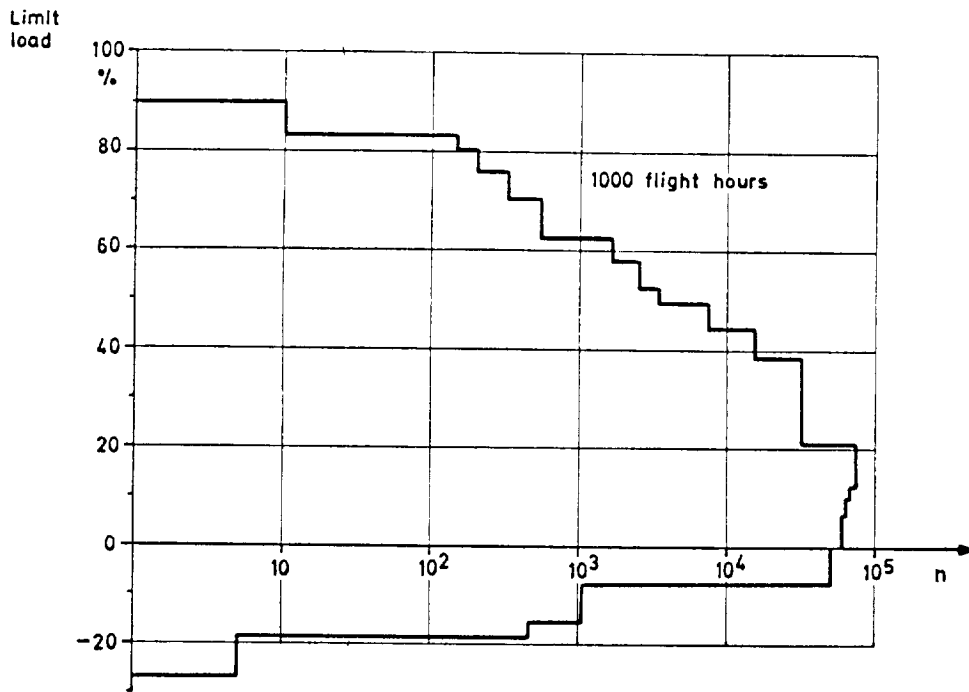


Figure 5.- The load spectrum used in testing.

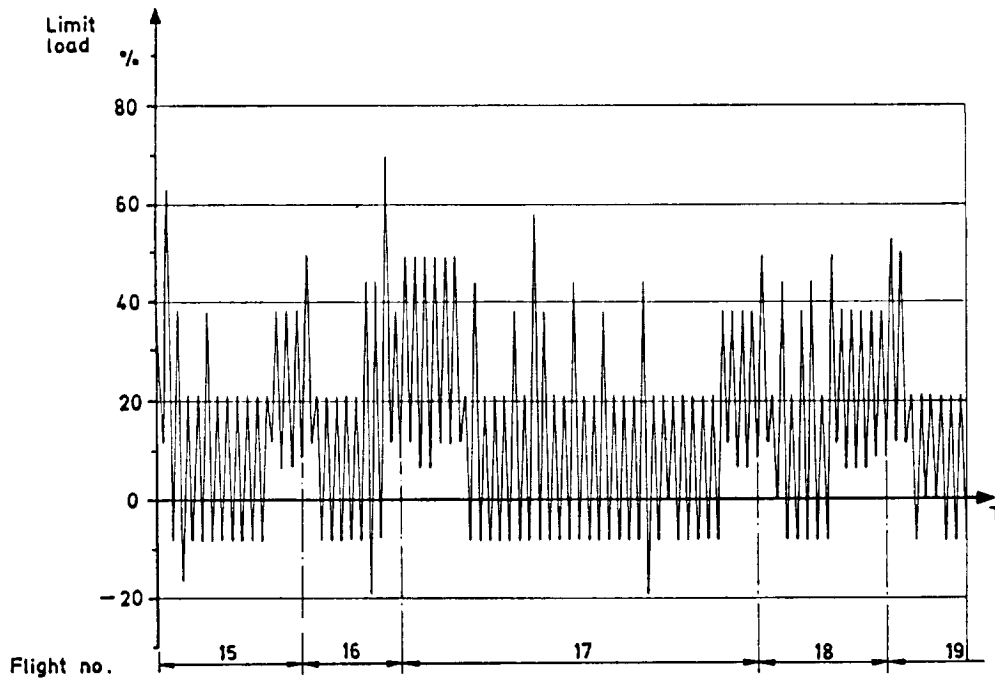


Figure 6.- Example of load sequences in the randomized flight-by-flight program.

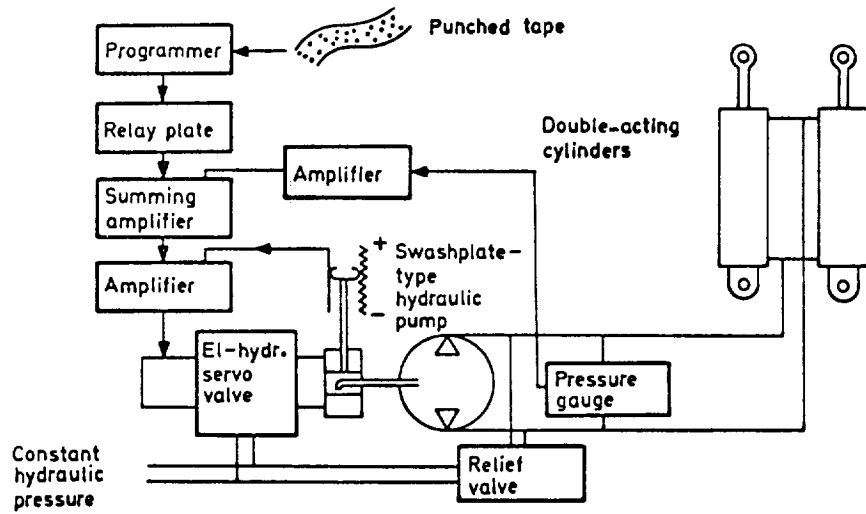


Figure 7.- Diagram of the test equipment system.

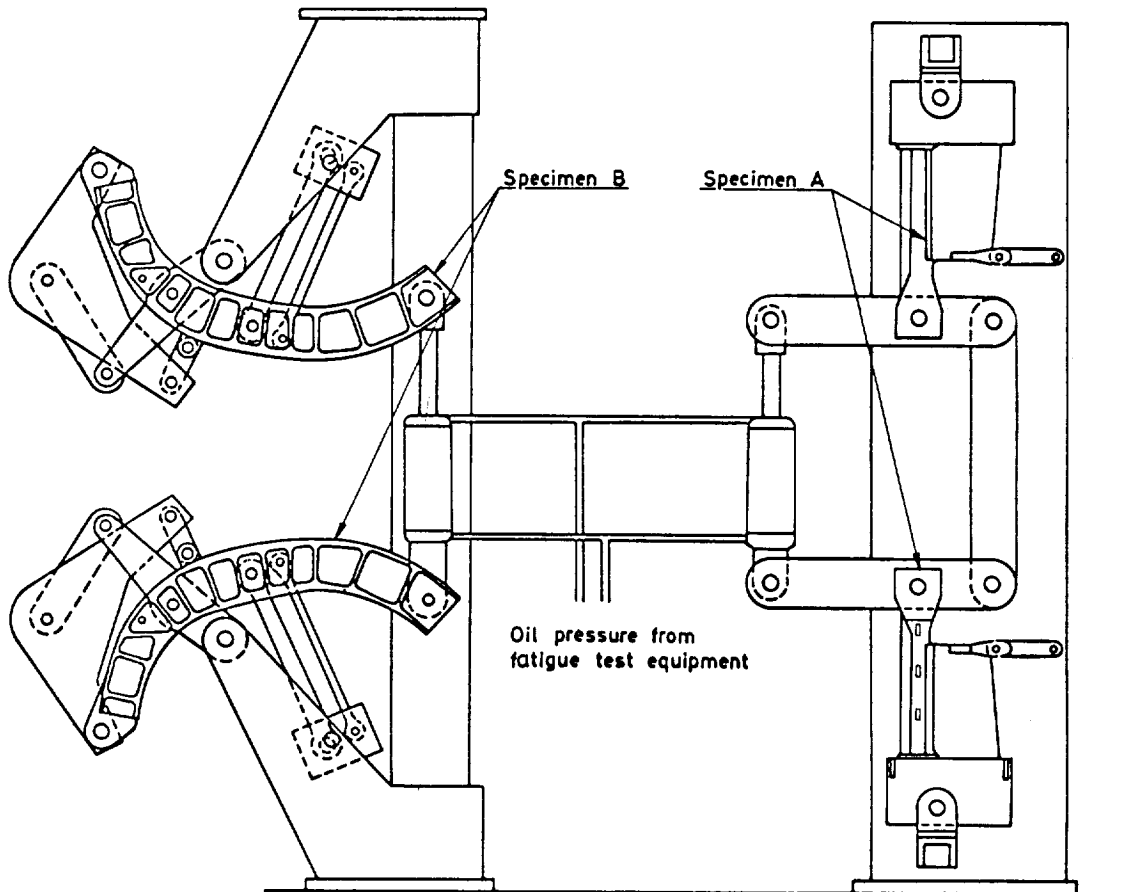


Figure 8.- Arrangement of test specimens.

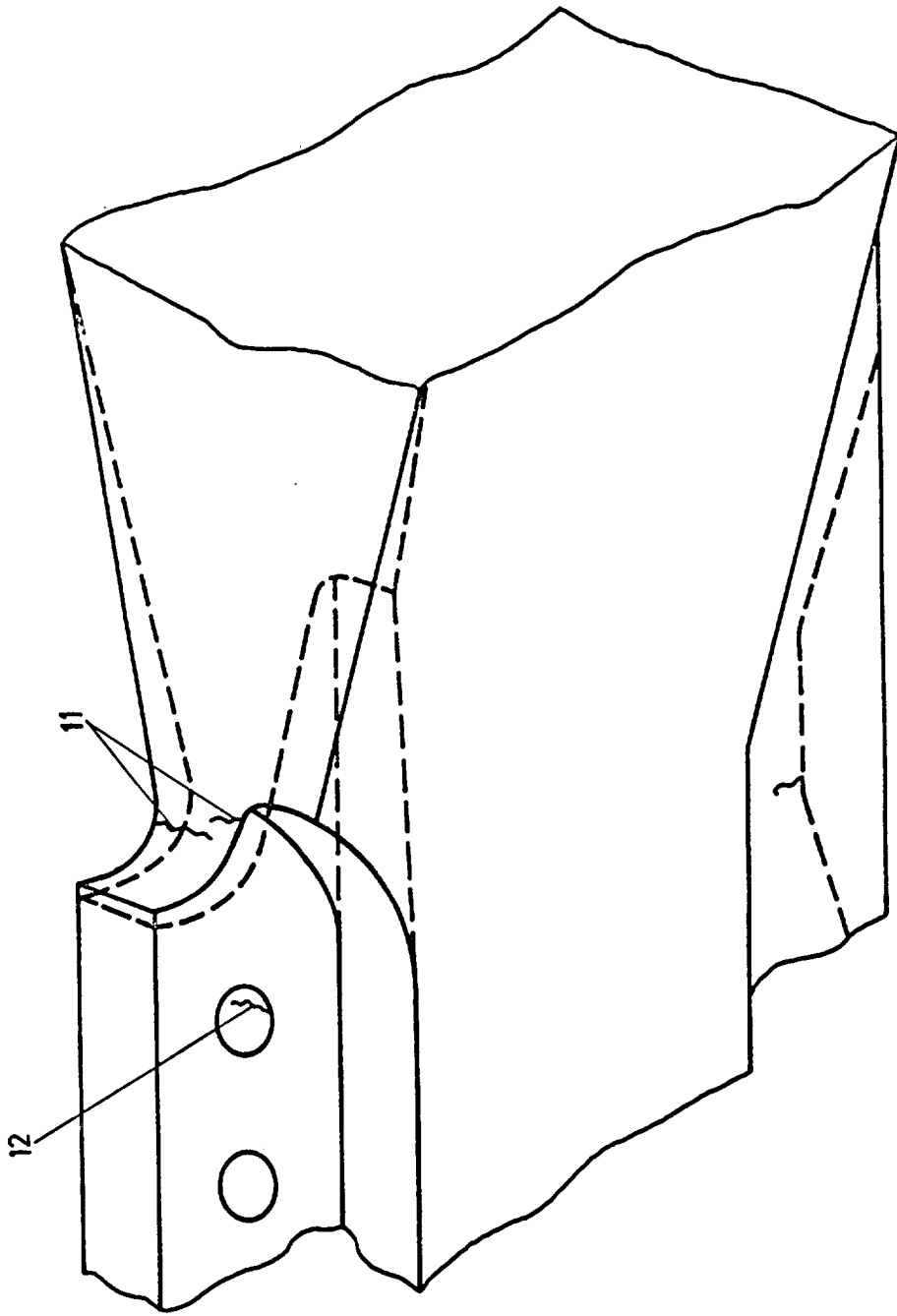


Figure 9.- Test specimen A₁ with cracks found. Solid lines indicate original specimen in which cracks 11 occurred. The cracked material was milled off and the shape of the specimen modified as shown by dashed lines before occurrence of crack 12.

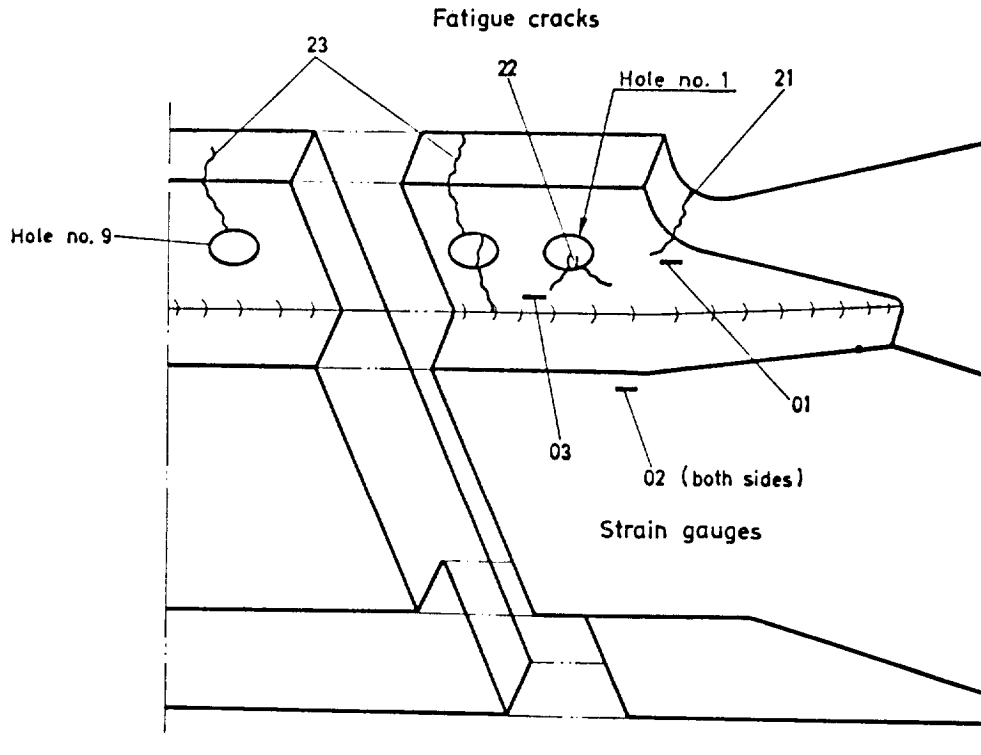


Figure 10.- Test specimen A₂ with cracks found.

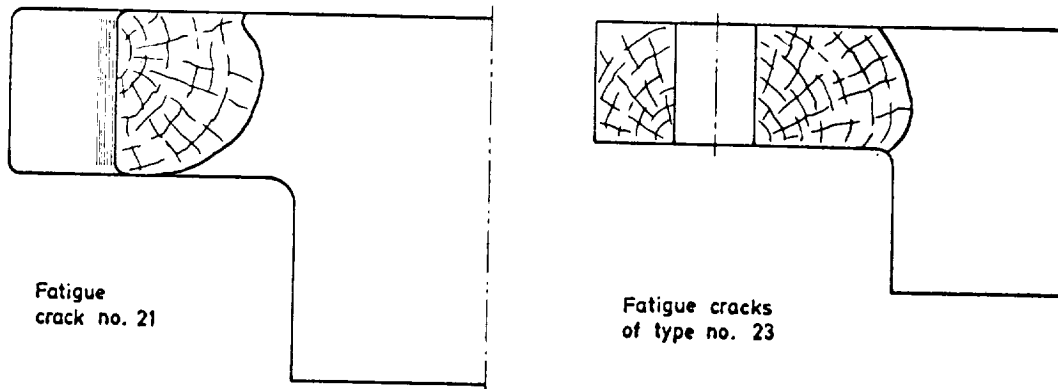


Figure 11.- Details of the cracked specimen A₂.

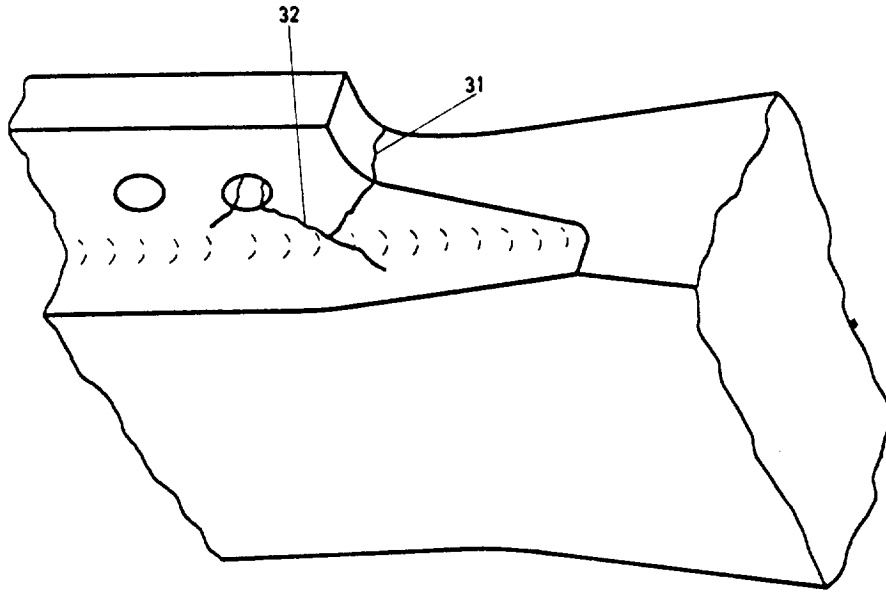


Figure 12.- Test specimen A₃ with cracks found.

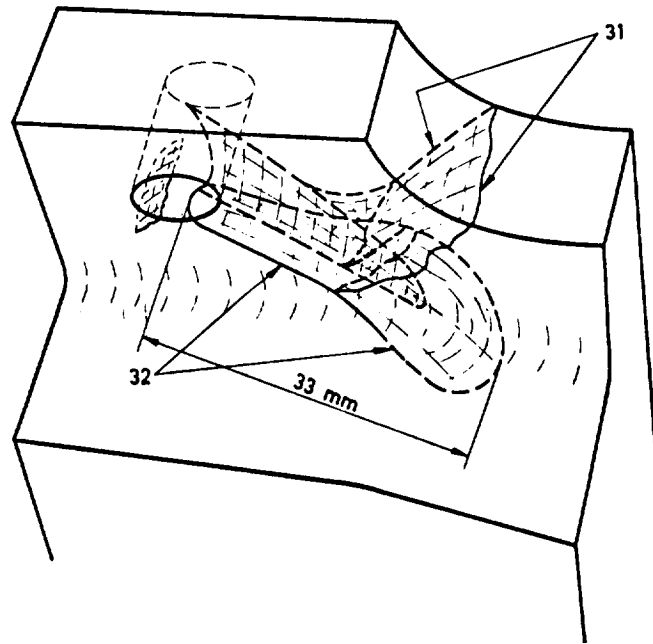


Figure 13.- Details of the cracked specimen A₃.

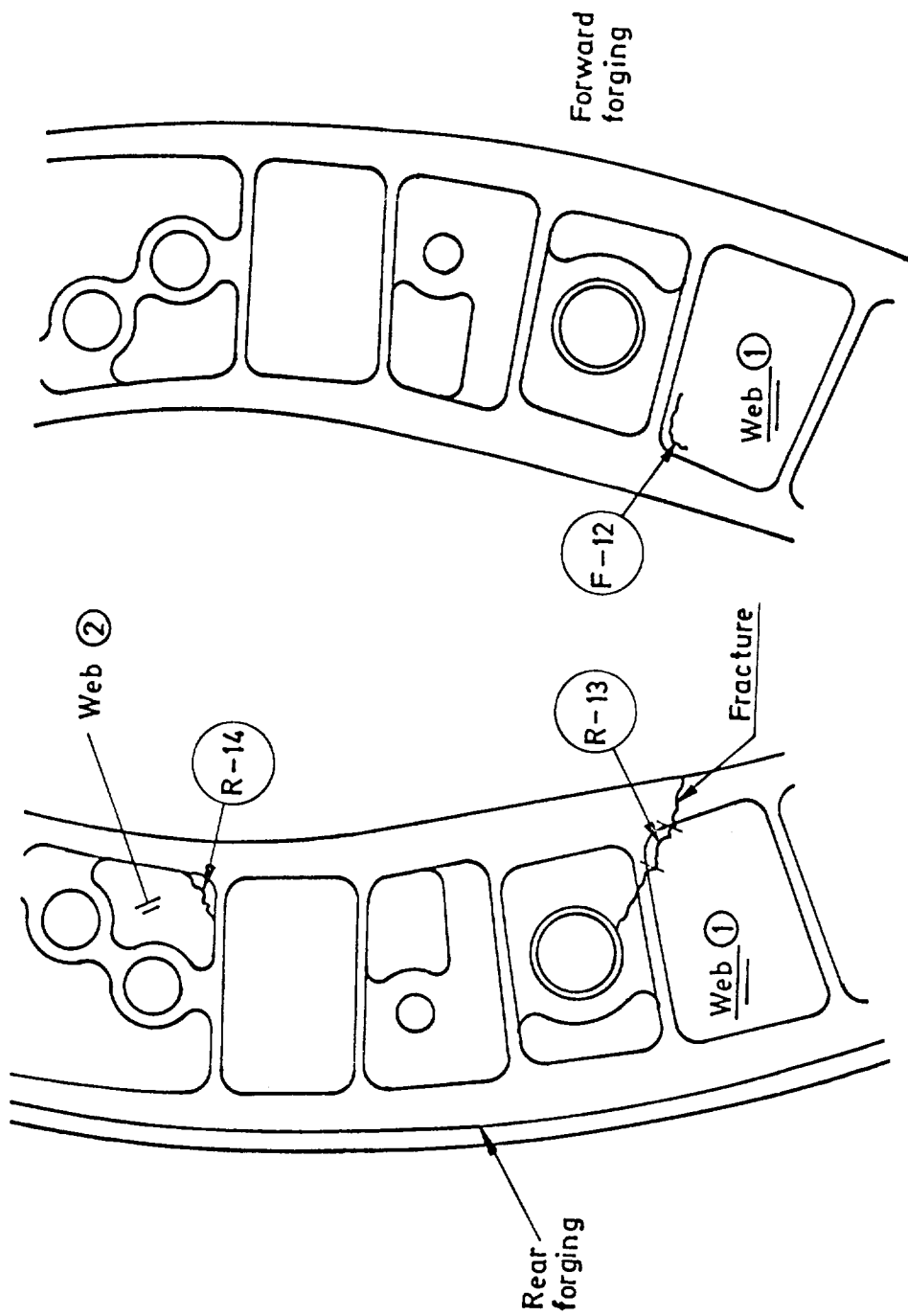


Figure 14.- Test specimen B1 with fatigue cracks and the location of failure indicated.

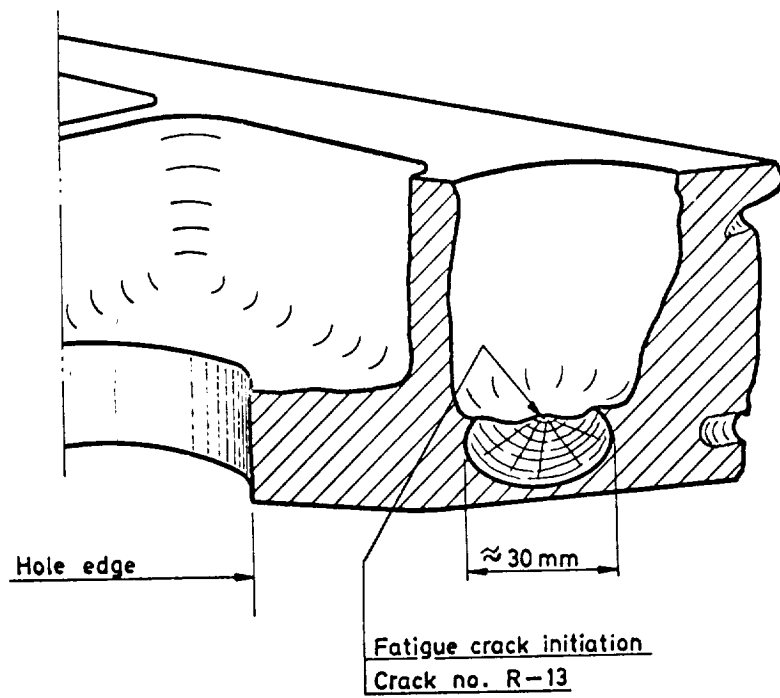


Figure 15.- Fractured area of specimen B₁.

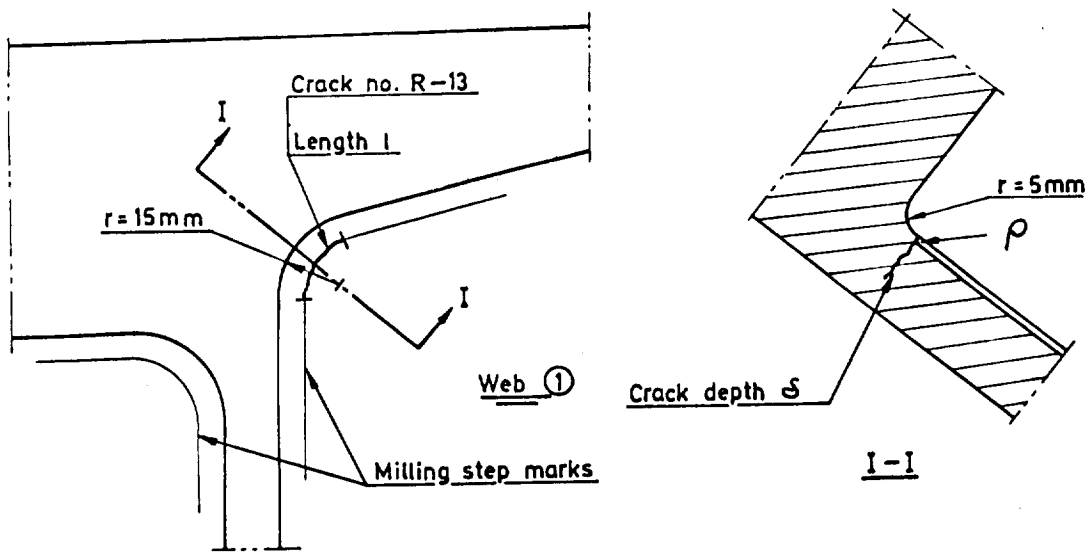


Figure 16.- The surface shape in a cracked area of specimen B₁.

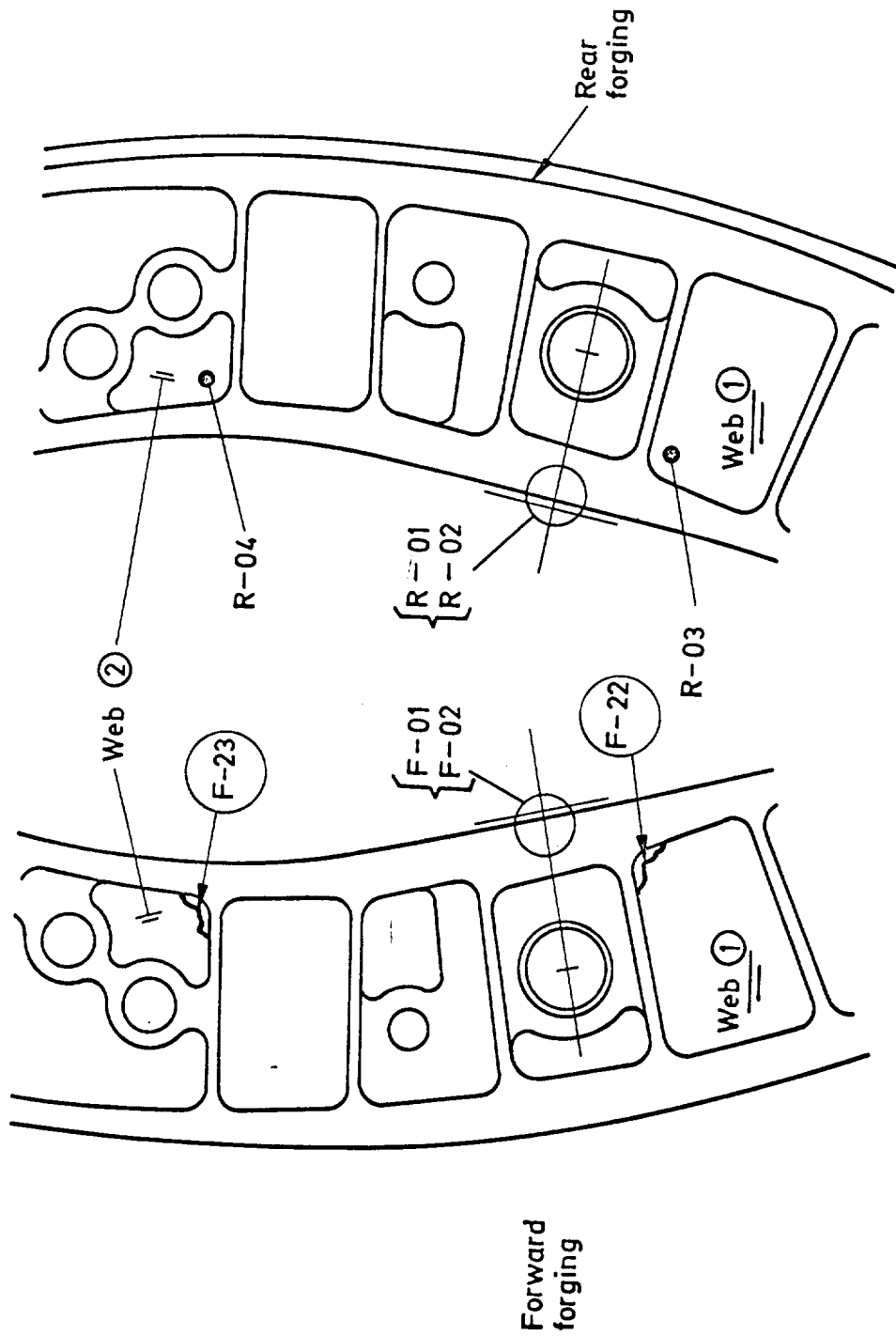


Figure 17.- Test specimen B₂ with cracks and location of strain gages indicated.

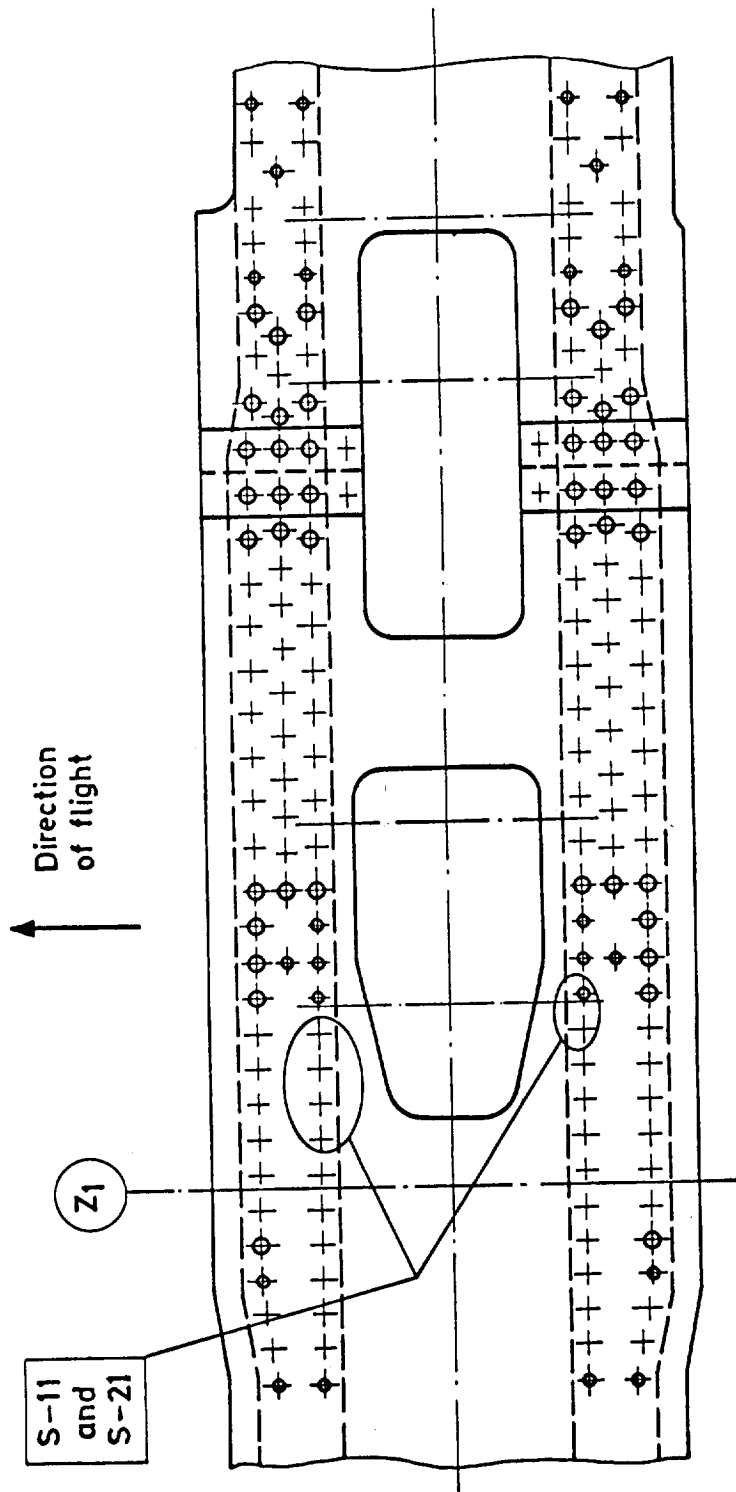


Figure 18.- Area with cracks in the inner sheet of the frame assembly. This figure represents both specimens B₁ and B₂.

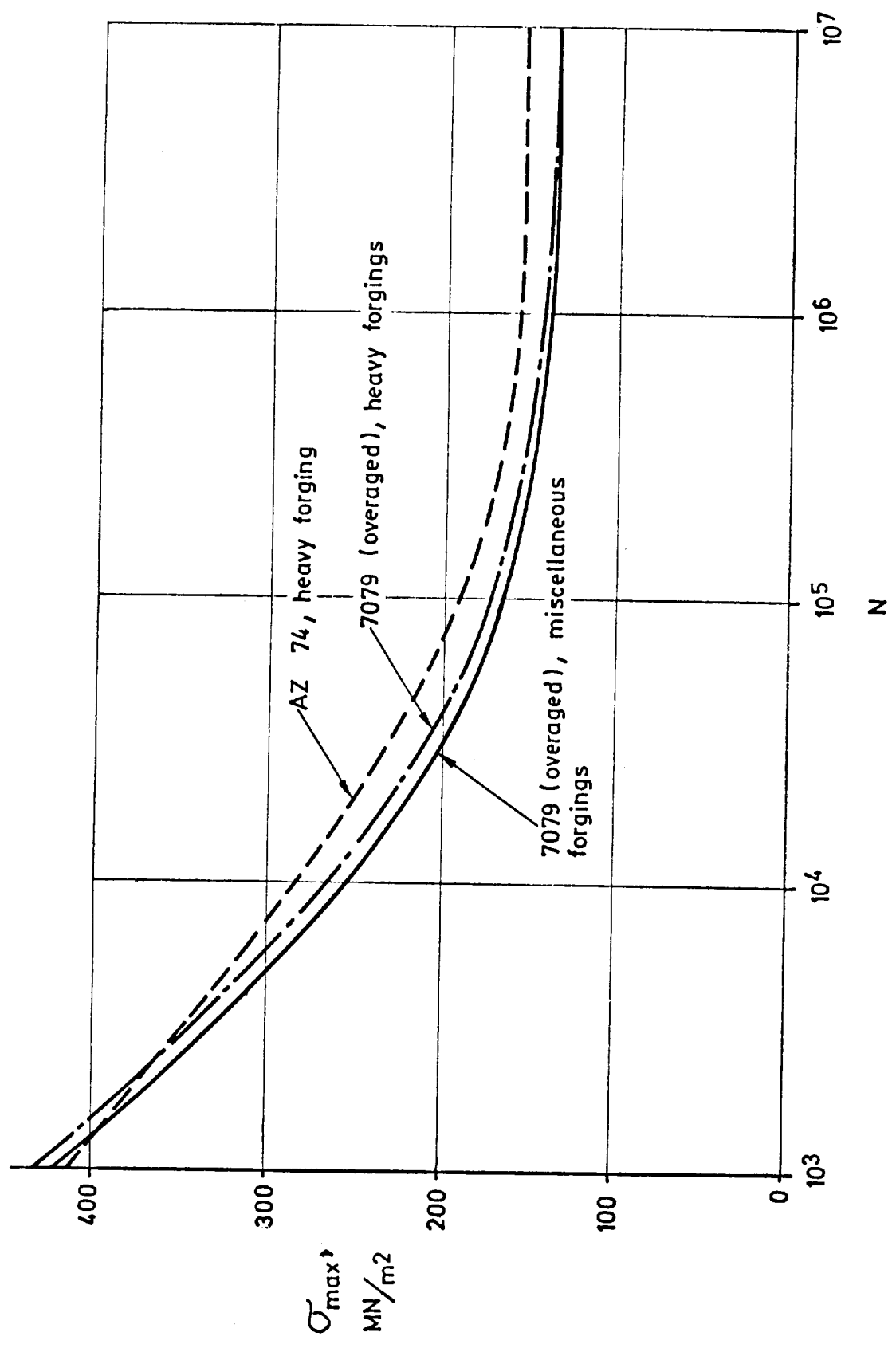


Figure 19.- Results of axial-load fatigue tests on notched round specimens. $K_t = 2.5$; $\sigma_{min} = 0$.

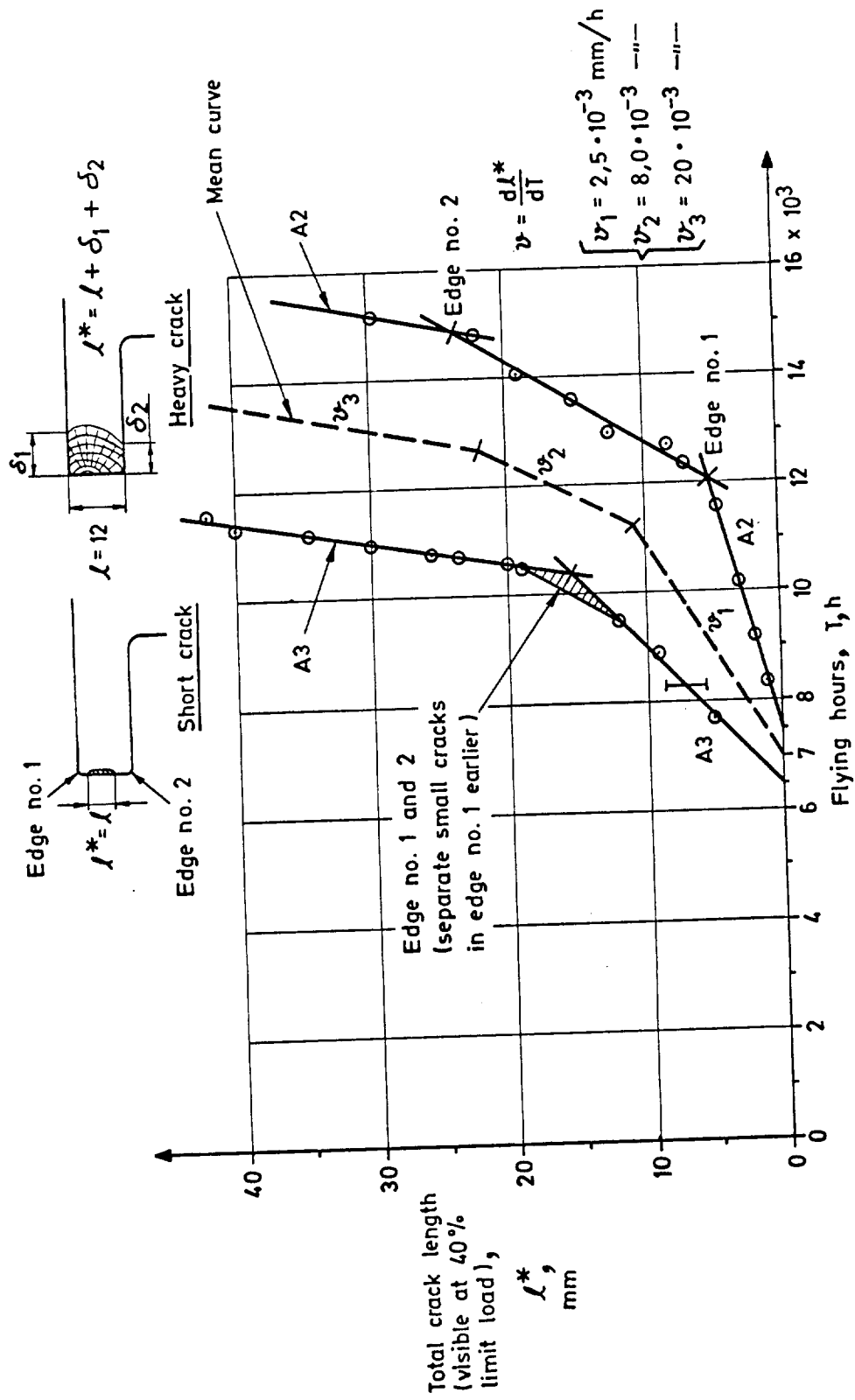


Figure 20.- Crack propagation at flange notch in specimens A2 and A3.

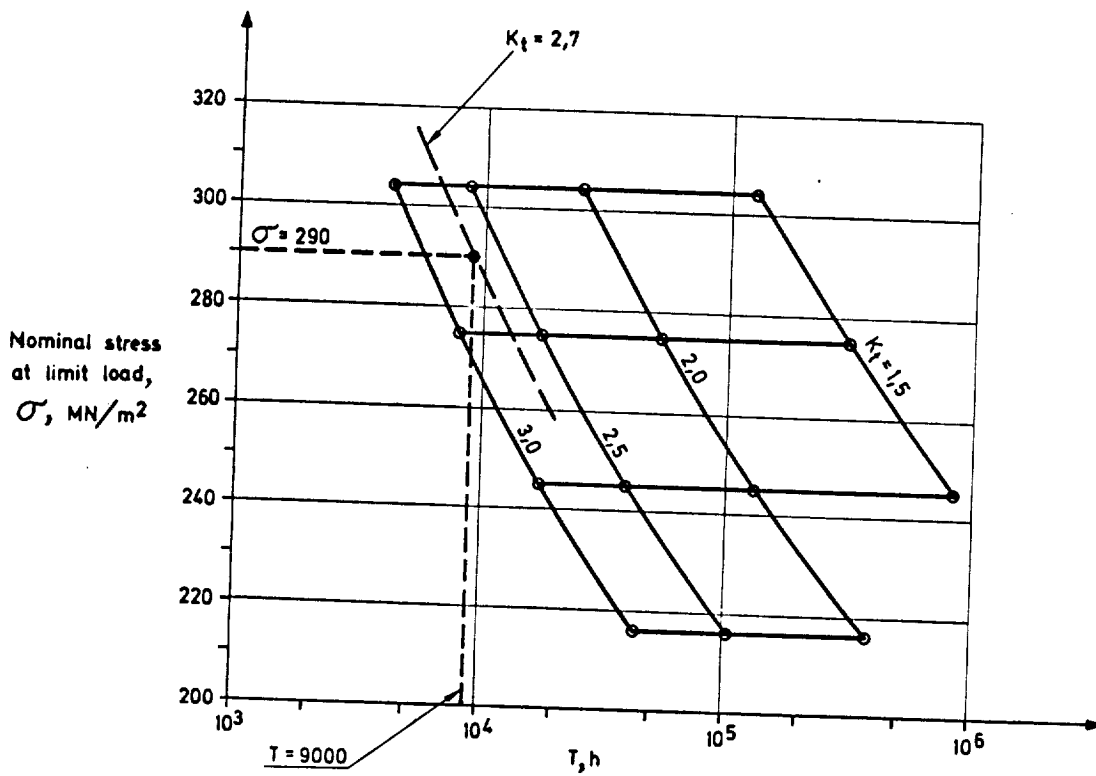


Figure 21.- Results of a cumulative damage calculation for specimen A material, AZ 74.

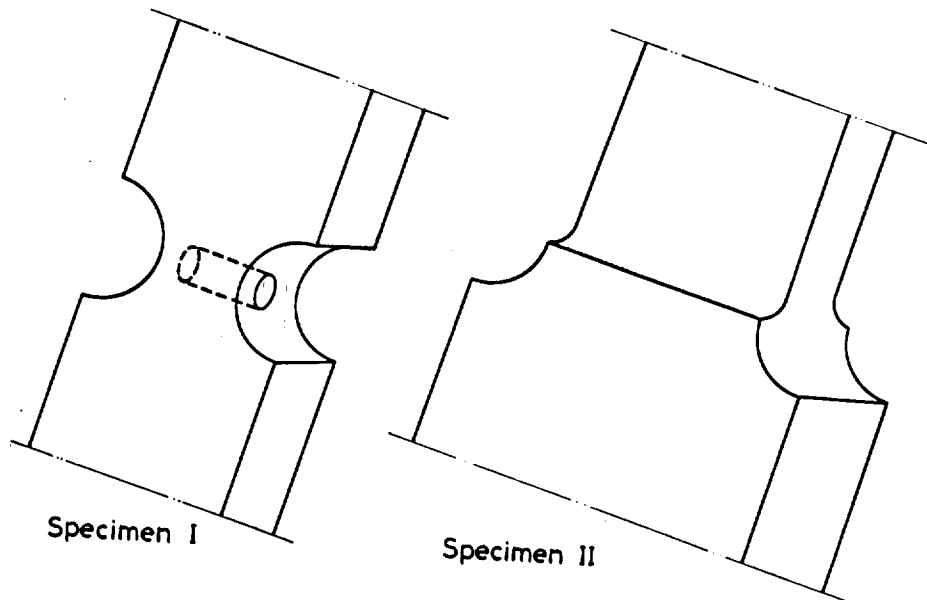


Figure 22.- Examples of interacting stress concentrations.